Computer Simulations For A Stochastic Theory Of Granular Drainage

R. Camilo Guáqueta

Submitted to the Department of Materials Science and Engineering in Partial Fulfillment of the Requirements for the Degree of

Bachelor of Science

at the
Massachusetts Institute of Technology

June, 2003

Signature of Author: ___ 05/19/03

Department Of Materials Science and Engineering
May 19, 2003

Certified By: ___ 5/19/03

Martin Bazant
Assistant Professor of Mathematics Thesis Supervisor

Accepted By: ___

Caroline A. Ross
Chairman, Undergraduate Thesis Committee

Computer Simulations For A Stochastic Theory Of Granular Drainage

by

Camilo Guáqueta

Submitted to the Department of Materials Science and Engineering in Partial Fulfillment of the Requirements for the Degree of Bachelor of Science

Abstract

There is a surprising lack of good models for granular flow. In 2002, Bazant proposed a new stochastic kinematic model of granular drainage from a silo. The new model rests on the notion that flow in the silo is caused by the migration of extended regions of excess interstitial space upward from the orifice at the bottom. An implementation of this model with the purpose of simulating the behavior of particles in the silo was developed by the author, and several results were obtained using simulations carried out with this implementation. As regards particle streamlines, average velocity profiles, predictions of particle mixing and of particle diffusivity, it was found that qualitative and quantitative agreement with experiments was excellent, in particular for a specific version of the implementation. This version uses a self-correlated random walk to describe the motion of the excess interstitial space through the silo.

The model can also be used to make predictions about many other features of the granular flow (such as granular temperature), that are not as accessible through experiments, and for which empirical behavior is not well known. In particular, the implementation of the model developed in this work can be used to simulate three dimensional flow, whereas existing experimental techniques are limited to observing two dimensions.

Thesis Supervisor: Martin Bazant
Title: Assistant Professor of Applied Mathematics

Contents

List of Figures

1 Introduction

We encounter the flow of granular materials such as gravel, sand, etc., over and again in industry and in daily life; from familiar devices such as hourglasses, to assembly-line hoppers that control the addition of fly ash to concrete. Surprisingly, though, granular flow is a poorly understood phenomenon. Even a relatively simple scenario, such as the drainage of granular material from a container, displays some interesting static and dynamic properties that are not predicted by existing models. While current models can correctly predict the average flow profiles of particles as they drain, they fail to predict the details of particle mixing. The lack of good models for granular flow can limit the development of new technologies and the optimization of existing ones.

Models for granular flow fall, very roughly, into three categories. The first kind are continuum models, which attempt to describe average properties of the flow with a few simple equations and assumptions. The second are computationally-intensive simulation techniques reminiscent of molecular dynamics [2] [8]. Finally there are also stochastic models which, although microscopic, do not attempt to tackle the physics of flow. Models of the first kind are not detailed enough and end up not providing sufficient useful information about the behavior of the particles. Models of the second kind, if anything, provide too much information, are too computationally intensive, and for all their complexity aren't very terribly successful. This leaves models of the third kind.

The only existing, reasonably successful stochastic model (known as the Void Model), makes largely inadequate predictions about several features of granular flow. In an attempt to correct these deficiencies, Martin Bazant proposed in 2002 a new stochastic model of granular drainage, which he provisionally dubbed the Spot Model. Preliminary analysis and simulations of granular drainage carried out with this model showed very promising improvements over the predictions of the Void Model. These initial simulations were implemented by Jaehyuk Choi, a graduate student

under Bazant, and were strictly two-dimensional, simplified versions of the Spot Model.

The research that lead to this thesis was the development of a more complete implementation of the Spot Model, that incorporates among other things the ability to simulate in three-dimensions. Generally stated, the goal of this research was twofold: first, simply to define what is necessary to implement the Spot Model, and second, to study some of the predictions this model makes about different aspects of granular drainage.

2 Experimental Procedures

Gathering data on the behavior of granular flow is in itself a daunting and complicated task. Because of this, it falls beyond the scope of this thesis to review existing experimental techniques, or to suggest improvements upon them. However, throughout the thesis, and particularly in section 5, I make reference and comparisons to some experimental results. In some cases these are well-established qualitative features, such as the parabolic shape of particle streamlines in drainage experiments. In other cases, however, I use detailed experimental velocity data obtained (in 2002) by Choi. It is worthwhile and relevant to give a brief explanation of how this data was generated.

A schematic of the experimental apparatus is shown in Figure (1). The container has clear walls, and its dimensions and the width of the hole can all be adjusted. However, D is always small compared to L. An experiment is run by plugging the orifice, filling the container with

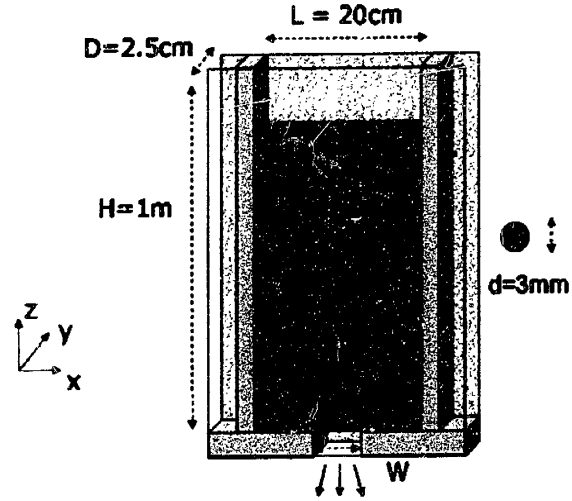

Figure 1: Experimental setup for granular drainage experiment, (image provided by Jaehyuk Choi.) The dimensions L and D are variable, as is the width of the hole. The particles are glass beads

particles (up to the desired height), and then opening the orifice to allow flow. Each experiment

is recorded with a high-speed video-camera, and then algorithms are applied to the results that make it possible to track individual particles and measure statistics concerning velocity, streamlines, velocity fluctuations, and so on.

An important feature of the experimental setup is that the results collected are essentially two-dimensional. Only the particles pressed up against the container wall can be observed, and since the wall constrains the lateral motion of those particles, it is likely that their behavior will differ from that of particles in the bulk. Moreover, the experiment itself is 2D in the sense that the container is so narrow in the y direction. At the time of this writing, I am not aware of any experiments that collect three dimensional data.

This has implications for any simulation of granular drainage. Despite the fact that a stated goal of my research was to make 3D simulation possible, I also had to develop a 2D limiting case in order to be able to meaningfully compare some of my results with experiment. The underlying assumption is that if a given choice of the free parameters in the model provides good agreement between the 2D simulation and the experiments, then the same choices will remain valid for the 3D simulation.

3 Theoretical Framework

There are essentially two existing models of interest for the problem of granular drainage from a container, which I will refer to here as the Continuum Kinematic Model (CKM) and the Void Model (VM). These two models, along with some experimental observations, provided the framework for the development of the Spot Model. The CKM is an analytical model that utilizes differential equations, and the VM is a stochastic model suitable for computer simulation. Both of these models are presented in some detail below.

3.1 Previous Models

3.1.1 Continuum Kinematic Model

The continuum kinematic model was developed by Nedderman and Tuzun [7]. As a continuum model, it presupposes that quantities such as density, velocity, and so on can be ascribed to each point in space in a well-defined way, and that generally they vary continuously. This is clearly not the case with granular materials, for which a quantity such as density only makes sense as an average over a finite volume. Nevertheless, the CKM succeeds in capturing some essential features of granular drainage. The model is based essentially on two assumptions. The first is that the granular material is incompressible. The second, that the mean horizontal velocity is proportional to the vertical shear rate. Formally, these assumptions are expressed as follows: Let $v(\vec{r})$ denote the mean vertical velocity of a particle at point $\vec{r}$, and $\vec{u}(\vec{r})$ denote the mean velocity in horizontal directions. Then the first assumption states

$$\nabla \cdot \vec{u} - \frac{\partial v}{\partial z} = 0 \tag{1}$$

where ∇ is an operation on horizontal dimensions only, and z denotes the vertical dimension. The second, constitutive assumption states

$$\vec{u}(\vec{r}) = b\nabla v(\vec{r}) \tag{2}$$

where b is a proportionality constant with units of length. This second assumption lacks a compelling microscopic justification, but nevertheless it expresses the physical intuition that particles will tend to drift laterally towards the regions with faster downward flows. If we combine equations (1) and (2), we obtain the central equation of the CKM:

$$\frac{\partial v}{\partial z} = b\nabla^2 v \tag{3}$$

This is essentially a diffusion equation, with b playing the role of a diffusion constant, and z playing the role usually played by time. This model is fairly good at predicting the mean flow profiles and streamlines for granular drainage well below the free surface. However, because it is a continuum model it has limited predictive power. It can only predict average quantities, not the behavior of individual particles. Thus, it cannot be used to study the details of particle mixing, or the behavior of the flow near boundary regions such as the free surface.

3.1.2 Void Model (VM)

The Void Model is based on the observation—first discussed by Litwiniszyn [4] and later refined by Mullins [5]—that the downward motion of particles in a granular material can be thought of as the upward motion of free space in the form of vacancies, or voids. Mullins deduced that the particle flux must be equal and opposite to the void flux, and formulated a stochastic model based on the upwards migration of voids [5]. In his model, the void motion has a strong upwards bias, and is

described by some probability distribution function (pdf). Also, a void's future path is assumed to be independent of its previous path. This model can correctly predicts, for granular drainage (although in a rather contrived manner), a diffusion length of two to three particle diameters, and parabolic streamlines. However, for similar reasons as the CKM, this model also has limited predictive power. What is really needed is a model that can track individual particles, which is what the VM provides. The VM is actually a special case of the more general theory developed by Mullins.

Caram and Hong independently developed the VM in 1991 [1]. They simplified Mullins' theory by assuming that the particles lie on a regular lattice, and by replacing the pdf for void motion with a biased random walk on this lattice (a severe restriction on void motion, as we shall see.) A particle moves by filling an adjacent void as illustrated in Figure (2).

These simplifications allow Mullins' theory to be transformed into a microscopic theory of granular

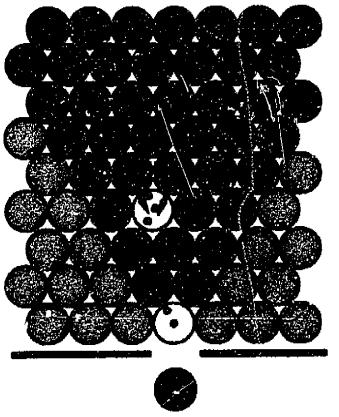

Figure 2: Illustration of how the VM works. Voids are inserted at the orifice and propagate upwards on the lattice by switching places at each step with one of the two higher adjacent sites. (Image provided by Martin Bazant.)

drainage. In other words, the VM actually makes predictions about the behavior of individual particles. It also makes it possible to specify void behavior at the boundary regions in order to

reproduce the different possible particle behaviors there. Caram and Hong implemented the VM as a computer simulation, using the two-dimensional triangular lattice illustrated above. They also specified that when a void reaches the free surface, it will continue to propagate along that surface, which produces a "cascading" effect on the surface particles. With this setup they were able to reproduce some key features of the flow, such as the stagnant region observed at either side of the orifice.

It is interesting to note that in the limit of long-time (that is to say, long z), and well away from any boundary regions, we can recover equation (3) from the VM. This is because for long z, the standard deviation of the lateral displacement of the voids is much larger than the lattice spacing, and therefore the asymptotics of the voids' random walks are described by a diffusion equation. In other words, if we let $c_{\mathrm{v}}(\vec{r})$ and $c_{\mathrm{p}}(\vec{r})$ denote the concentration (i.e. probability density) of voids and particles, respectively, at point $\vec{r}$, then $c_{\mathrm{p}} = c_{\max} - c_{\mathrm{v}}$ (where $c_{\max}$ is the maximum particle concentration), and the long z behavior satisfies:

$$\frac{\partial c_{\mathrm{v}}}{\partial z} = b\nabla^2 c_{\mathrm{v}} \tag{4}$$

The particle and void fluxes are equal and opposite, so $c_{\mathrm{v}} v_0 - c_{\mathrm{p}} v = 0$, where v_0 is the constant vertical velocity of the voids. If we assume the void concentration to be low, then $c_{\mathrm{p}} \approx c_{\max}$, which implies

$$c_{\mathrm{v}} = -v\frac{c_{\mathrm{p}}}{v_0} \approx -v\frac{c_{\max}}{v_0}$$

Plugging this relation back into Equation (4) we obtain Equation (3). Because of this, we see that the VM makes approximately the same predictions for mean flow that the CKM does.

For the VM, the parameter b is the lateral diffusion length of both voids and particles. Since the void motion is restricted to lie on a lattice, the choice of lattice determines b. It can be shown that

for a face-centered cubic lattice, $b = r_p/2\sqrt{(6)}$, and for a body-centered cubic lattice, $b = r_p/2\sqrt{(2)}$, where r_p is the particle radius [3].

3.1.3 Discussion of VM, CKM – idea for SM

Both the CKM and the VM make correct predictions for the average velocity profiles and average streamlines. That is, we can derive from Equation (3) that on average, the paths followed by particles as they leave the container are parabolic. However, if we observe the individual particle paths predicted by the VM (obtained from the computer simulation), we see that they differ widely from this prediction. The Void Model predicts that the lateral diffusion length of the particles is equal to that of the voids, which leads to far more particle mixing than predicted by the CKM or observed in experiments. This gross overestimation of particle diffusivity and mixing is perhaps the greatest problem with the VM. Another problem is underestimation of the void diffusivity: Any reasonably close-packed choice of lattice leads to $b < r_p$, but experiments have consistently shown $b > r_p$.

The Void Model also fails to incorporate an important characteristic length scale. This length scale is observed experimentally in at least two ways. Firstly, it is well-known that in granular drainage no flow will occur unless the orifice is at least three particle diameters wide. This is because of a phenomenon called arching, in which several particles trying to leave the container at once will jam and make an arch that prevents further flow. Secondly, Bazant [3] demonstrated that empirically, there is a strong correlation in the velocity of particles that are within about three particle diameters of each other. It is possible, as well, that this length scale describes the width of some boundary layers, such as that of reduced flow near a rough wall. These phenomena are not reproduced or accounted for by the VM, and there seems to be no obvious way to correct this.

Motivated by the observation of a missing length scale, and by the failure of the VM to correctly

predict particle mixing, Bazant proposed a new theory for granular drainage [3] [2], the Spot Model. The basic idea behind the SM is to replace voids, which are particle-sized vacancies in a lattice, with 'spots', which are more extended regions of slightly smaller particle density. The Spot Model is described in more detail in the next section.

3.2 Description of the Spot Model

Replacing vacancies with regions of lower density (or alternatively, excess interstitial space) leads to a new stochastic, microscopic model for granular drainage. Like the VM, the SM can make predictions about individual particles, but an added advantage of replacing voids with spots is that the motion of the spots is not constrained to lie on a specified lattice. The particles can lie in a random close-packed arrangement and the spots can follow a random walk or Brownian motion through this arrangement without any ambiguity as to which particles are to be moved. This is not only a more physically realistic picture of what takes place inside the container, but also allows for exact matching of the parameter b to experiments, by tailoring the motion of the spots. Additionally, the spot (b) and particle (b_{p}) diffusivities can differ, which was not possible in the VM.

As a spot moves in a given direction, the particles that pass through it undergo a displacement in the opposite direction, as illustrated by Figure (3). The spot is an extended region, so as it moves it affects several particles at the same time. Because of this, the velocity of these particles will be strongly correlated. Thus, the SM can incorporate the missing length scale discussed in the previous section: by picking the radius of the spot, we can pick the extent of the particle-particle velocity correlations. Furthermore, if we assume that spots are incompressible then we also recover the length scale at the orifice, because incompressible spots cannot enter the container unless the orifice is at least as large as they are. On both accounts the experimental evidence strongly suggests

that a spot's effective diameter should be about three particle diameters, the same as the missing length scale.

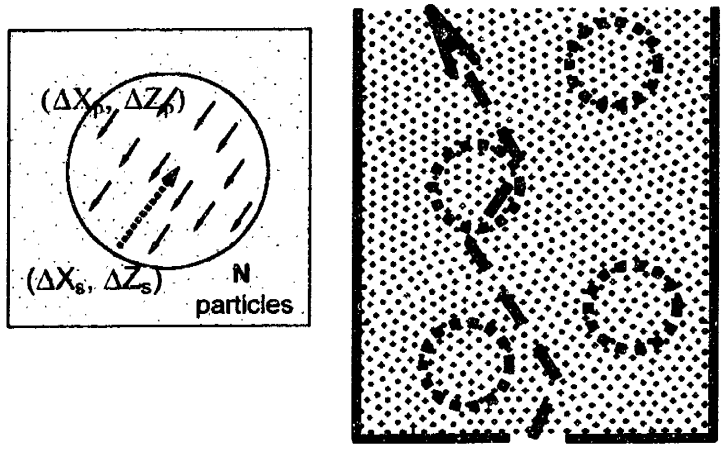

Figure 3: Illustration of the SM. Spots are inserted at the orifice and propagate upwards, moving particles as they go along. (Image provided by Martin Bazant.)

To determine the details of how individual particle displacements are caused by a spot, Bazant introduced the notion of a spot influence function, which I will denote $w(\vec{p}_s, \vec{p}_p)$, where $\vec{p}_s$ and $\vec{p}_p$ are the position vectors of the spot and the particle, respectively. This function describes the shape and extent of the spot. For example, a spherically symmetric spot implies $w(\vec{p}_s, \vec{p}_p) = \psi(|\vec{p}_s - \vec{p}_p|)$. The information contained in $w(\vec{p}_s, \vec{p}_p)$ is also necessary to impose the constraint that particle and 'void' fluxes be equal. In the case of the SM, the equality must hold between the flux of particles and the flux of excess interstitial volume carried by the spots, and $w(\vec{p}_s, \vec{p}_p)$ describes how the former is caused by the latter. In addition, we must also specify the amount of excess volume a spot carries, which I denote Ω_s. Following Bazant, I will conveniently express Ω_s in term of particle volumes, so that

$$\Omega_s = \alpha V_p = \alpha \left(\frac{4}{3} \pi r_p^3 \right)$$

i.e. α is the number of particle volumes worth of excess space carried by a spot. Although the VM sets $\alpha = 1$ by default, intuitively it seems more realistic to assume $\alpha \ll 1$, and this intuition is borne out by experimental results.

It is interesting to note that in a way, the SM is a generalization of the VM, which relaxes some of the restrictive assumptions of the latter. This can be seen in the fact that the VM can be recovered as a special case of the SM, which can be done if we take $\alpha = 1$, set the spot radius r_s equal to the particle radius, specify the motion of the spots as a random walk on a lattice, and use the influence function

$$w(\vec{p}_s, \vec{p}_p) = \psi(|\vec{p}_s - \vec{p}_p|) = \psi(r) = \begin{cases} 1 & \text{if} \quad r \leq r_s \\ 0 & \text{if} \quad r > r_s \end{cases} \tag{5}$$

4 Implementation

The Spot Model can very naturally be implemented as a discrete computer simulation. By 'discrete' I mean that the spot motion is described by a directed random walk with discrete steps, rather than by continuous Brownian motion. However, just as a choice of lattice has to be made to implement the VM as a simulation, there are choices of algorithms and parameters that have to be made in order to translate the Spot Model into computer code. The following sections described the choices I made to obtain my implementation.

4.1 Basic Setup

The container in which the simulations take place is a box with dimensions, (W, L, H), that can be specified arbitrarily. The location ($\vec{p}_{\mathrm{h}}$) and radius (r_{h}) of the orifice can also be specified for each simulation run. The particles initially fill the container in a face-centered cubic (FCC) lattice. This lattice was chosen for simplicity's sake, since no simple algorithms exist to produce a random close packed arrangement. Furthermore, the packing fraction of the FCC lattice is close to that of a random close packing. Since the spots are not restricted to this lattice the choice of lattice is not as important as it would be in the VM.

Spots are created in groups of $1/\alpha$, so that an event of spot creation corresponds to one particle volume leaving the container. They are created and injected into the container every κ timesteps. This parameter could be used to control the absolute value of the particle velocity, and is presumably largely determined by the width of the orifice. However, as explained in section 4.5, I chose to ignore these dynamics concerns. Thus, for all results presented in this thesis I used $\kappa = 1$, since this speeds up the running time of the simulations. α was also somewhat arbitrarily picked to be equal to $1/2$.

At every timestep, the displacement each spot took in the previous timestep is used to compute the corresponding particle displacements. Then, each spot in the container is advanced one more

step along its random walk.

4.2 Influence Function

Two important choices that have to be made to obtain a computer simulation of the spot model are the choices of spot radius and influence function. These choices are closely related to each other. It is possible, in the abstract, to have a spot of infinite extent described by—for example—a Gaussian influence function. It is also possible to have a non-spherically symmetric spot. In these cases it becomes necessary to think in terms of an effective spot radius, or an average spot radius. Moreover, to simulate a spot of infinite extent in a computer, we also have to pick some cutoff value for the influence function beyond which it is zero. I call this cutoff value the interaction, or influence, range r_{inf}.

For my implementation, I chose the very simple influence function given by Equation (5). Since in this case $w(\vec{p}_{\text{s}}, \vec{p}_{\text{p}}$ is a square function, there is no ambiguity about the meaning of r_{s}. From the experimentally observed length scale of three particle diameters, I (somewhat arbitrarily) chose $r_{\text{s}} = 7r_{\text{p}}$. There are two main reasons why I did not choose other, more complex influence functions. Firstly, as noted by Bazant, the influence function is a powerful tool in the SM because it describes in great detail the effect of a spot on particles. For example, different (even perhaps location-dependent) choices of w could conceivably be used to account for the behavior of particles in boundary layers or in regions of highly non-uniform flow. Thus, the influence function deserves a great deal of study that is beyond the scope of this present work. The second reason that I chose a simple w is that as it turns out, it can significantly affect the running time of the simulation. The influence function is evaluated at every timestep, for every particle that is within the interaction range of a spot, which for any sizeable simulation amounts to millions of evaluations.

4.3 Computing particle displacements

The fact that the particle displacements at timestep t are computed using the spot displacements from timestep $t-1$ is due to the fact that the particles cannot move until they are actually in the region of lower density. (In reality, of course, both flows occur simultaneously.) Given the spot displacements at $t-1$, the corresponding particle displacements are computed as follows:

Let $\vec{d}_{\mathrm{s}}$ be the displacement of a spot in the previous timestep, and $\vec{d}_{\mathrm{p}}^{(i)}$ be the displacement that this spot induces on the i^{th} particle in the current timestep. The constraint that the total flux of particle volume be equal and opposite to the flux of excess interstitial volume translates to the following constraint on the displacements vectors:

$$\sum_{i \in \mathbb{S}} \vec{d}_{\mathrm{p}}^{(i)} = -\alpha \vec{d}_{\mathrm{s}} \tag{6}$$

where $\mathbb{S} = \{i : |\vec{p}_{\mathrm{s}} - \vec{p}_{\mathrm{p}}^{(i)}| < r_{\mathrm{s}}\}$ is the set of all particles within the spot's radius. Furthermore, because $i \in \mathbb{S}$ implies that $w(\vec{p}_{\mathrm{s}}, \vec{p}_{\mathrm{p}}) = 1$, Equation (6) simplifies to:

$$|\mathbb{S}| \vec{d}_{\mathrm{p}} = -\alpha \vec{d}_{\mathrm{s}} \tag{7}$$

where $\forall i, \vec{d}_{\mathrm{p}}^{(i)} = \vec{d}_{\mathrm{p}}$. Since recomputing $|\mathbb{S}|$ for every spot at every timestep would be computationally quite costly (because it requires evaluating $|\vec{p}_{\mathrm{s}} - \vec{p}_{\mathrm{p}}|$ so many times), I assume in my implementation that $|\mathbb{S}|$ is constant and equal to the average number of particles that can fit in a spot, so that $|\mathbb{S}| = \phi(r_{\mathrm{s}}/r_{\mathrm{p}})^3$, where $\phi \approx 0.74$ is the volume fraction of particles in an FCC lattice.

4.4 Random Walks of Spot Motion

Clearly, the behavior of particles in the simulation will be heavily dependent on the details of the random walk taken by the spots. Through computer simulation, I studied the behavior of the model under three different types of random walks.

For any random walk the spot takes, the displacement vector of the spot at timestep t is given by:

$$\vec{d_s}(t) = x_t\hat{\imath} + y_t\hat{\jmath} + z_t\hat{k} \tag{8}$$

where x_t, y_t, and z_t are random variables with a specified distribution. All three random walks I considered have a constant vertical displacement $z_t = \Delta z$, and a constant waiting time of one timestep between successive steps. Thus, the random walks differ only in the probability distributions of the horizontal components of $\vec{d_s}(t)$. In each case, these distributions were constrained so that the lateral diffusivity of spots was equal to the experimentally obtained value[1]:

$$b = 1.3r_p \tag{9}$$

Since in physical reality the spots move continuously, the parameter Δz is an artifact that comes about from simulating the model discretely. Thus, the value of I chose for my implementation was chosen somewhat arbitrarily. Presumably, the smaller Δz is, the more the discrete random walks will resemble paths taken by real spots. However, a decrease in Δz is also accompanied by an increase in running time. To determine a suitable value, I ran simulations with progressively smaller values of Δz and stopped when the results were essentially no longer changing. What I found is that for values smaller than about $r_p/2$, changes in Δz have no discernible effect on the

[1]This particular value was obtained by Choi using the experimental setup described in section 2

outcome of the simulation. I accordingly chose a value $\Delta z = r_p/3$, which is the value I use for all other results presented in this thesis.

The three different types of random walks I studied are described in the following subsections.

4.4.1 Conical Distribution (CD) Random Walk

In this type of random walk, the random variables x_t are independent and identically distributed for all t, and similarly for the y_t, so we can drop the subscripts. Let R be a uniformly distributed random variable between 0 and ρ, and θ be a uniformly distributed random variable between 0 and 2π. Then x and y are given by:

$$\begin{aligned} x &= R\cos(\theta) \\ y &= R\sin(\theta) \end{aligned} \tag{10}$$

Thus, the probability distribution of x and y on the plane is a cone centered on the position of the spot, with base radius ρ. To satisfy Equation (9) we use the result from random walk theory [3] that

$$b = \frac{\langle|\vec{h}|^2\rangle}{2d\Delta z} \tag{11}$$

where $\vec{h} = x\hat{\imath} + y\hat{\jmath}$, d is the number of horizontal dimensions (equal to two in this case), and $\langle . \rangle$ is the expected value. Since

$$|\vec{h}|^2 = x^2 + y^2 = R^2(\cos(\theta) + \sin(\theta)) = R^2$$

and

$$\langle R^2 \rangle = \rho^2$$

it follows that

$$b = \frac{\rho^2}{4\Delta z}$$

Thus, Equation (9) implies that $\rho = \sqrt{5.2 r_p \Delta z}$.

This is the random walk I originally picked for my implementation, and most of the exploratory work with the model was carried out using a CD random walk. It was only until the implementation was otherwise complete that I incorporated, for reasons of mathematical nicety, the two other random walks detailed below.

4.4.2 Bivariate Normal (BN) Random Walk

As with the CD random walk, the x_t's and y_t's are independent and identically distributed for all t. They are also independent of each other. Both x and y have a normal, or Gaussian, distribution with mean 0 and variance σ^2. Since

$$\langle |\vec{h}|^2 \rangle = \langle x^2 + y^2 \rangle = \langle x^2 \rangle + \langle y^2 \rangle = 2\langle x^2 \rangle = 2\sigma^2$$

it follows from Equations (9) and (11) that $\sigma = \sqrt{2.6 r_p \Delta z}$

The Central Limit Theorem of probability [9] states that the probability distribution of a sum of independent random variables approaches a normal distribution. The motion of spots can be thought, physically, to be the collective result of many small motions of particles, each of which is randomly distributed. Thus, it seems natural to pick a normal distribution for the random walk taken by the spots.

4.4.3 Correlated Bivariate Normal (CBN) Random Walk

The third kind of random walk that I studied is slightly more complicated than the previous two. This is because the x_t's and y_t's are no longer independent, although they continue to be identically distributed. Both x_t and y_t have the same distribution as in the BN random walk, with the same value of σ. However, now we impose the further constraint that the correlation between x_t and x_{t-1} be equal to a new parameter, γ. Satisfying this constraint is particularly easy because x_t is normal and sums of normal variables are also normal. Let x_R be a normally distributed random variable with mean 0 and variance 1, independent from x_t for all t. Then the desired relation between x_t and x_{t-1} is

$$x_t = \gamma x_{t-1} + \beta x_R \tag{12}$$

To see this, we use the definition of correlation:

$$\mathrm{Corr}(x_t, x_{t-1}) = \frac{\langle x_t x_{t-1}\rangle - \langle x_t\rangle\langle x_{t-1}\rangle}{\sigma^2}$$

The mean of x_t is zero, so

$$\sigma^2 \mathrm{Corr}(x_t, x_{t-1}) = \langle x_t x_{t-1}\rangle = \gamma\langle x_{t-1}^2\rangle + \beta\langle x_{t-1} x_R\rangle \tag{13}$$

Since x_{t-1} and x_R are independent, it follows that the second term is zero. By definition, $\langle x_{t-1}^2\rangle = \sigma^2$, and thus we see that $\mathrm{Corr}(x_t, x_{t-1}) = \gamma$, as desired. We also wish to insure that $\langle x_t^2\rangle = \sigma^2$, and this gives the relation on β:

$$\langle x_t^2\rangle = \sigma^2 = \gamma^2\sigma^2 + \beta^2$$

implies

$$\beta = \sqrt{\sigma^2(1-\gamma^2)}$$

The overall effect of correlating consecutive steps in the random walk is that the spot will change direction more smoothly; each step can be thought of as a weighted average of the previous step and a random component.

4.4.4 Two-dimensional case

Because of the way experimental results are collected, I decided to incorporate, as well, the ability to run simulations in two dimensions. However, there is some ambiguity about how this should be done. In my implementation I assume that spots are incompressible, but clearly since flow occurs in containers of width less than $2r_s$, this assumption is not always valid. Since no theory exists for how spots behave when the container width is smaller than $2r_s$, and developing such a theory is beyond the scope of this work, I chose to run my 2D simulations by setting $W = 2r_s$. The assumption of incompressibility implies in this case that the y motion of the spots will be completely restricted. Thus, when I say a simulation is 2D, I don't mean that the simulated medium is two dimensional (as in the VM implementation of Caram and Hong), but rather that $y_t = 0$ for all t.

In general, one might expect that, to maintain the validity of Equation (9) the distribution of the x_t's would have to be scaled, since now $\vec{d}_s(t) = x_t\hat{\imath} + \Delta z\hat{k}$. A useful feature of using normal random variables, however, is that it turns out that the desired value of σ is the same in both 2D and 3D cases.

4.5 Dynamics

In the simulation, time is measured only in terms of timesteps, or in other words algorithm steps. Presumably, if the dynamical properties of the simulation were appropriately defined, then it would

be possible to translate timesteps into real time units. This would enable the computation of real-unit velocity magnitudes and other temporal information from simulations. However, Bazant [3] made the observation that achieving this would require the introduction of a few more parameters into the model. The mean flow rate of the spots, and the amount of interstitial volume they carry, Ω_s, would have to be matched to experimental observations. Also, interactions between spots would have to be considered. Finally, we could no longer assume a constant waiting time between successive steps of a spot's path. Because of these many complications, I chose not to attempt to define the dynamics of the simulation. Thus, temporal data that I obtain from simulation cannot be directly compared to experimental results.

4.6 Data available

Both for experiments and simulations, there are two fundamentally different ways of measuring the velocity of particles in the container. The first is to follow each particle along its path, keeping track of its displacements at each timestep. This method yields precise knowledge about each particle's velocity. The second method is to conceptually divide the container into little boxes, and keep track of the particle displacements that take place inside each box. This method yields the average velocity at different points in the container. Although the second method is more commonly used, there are advantages and disadvantages to either one.

One of the powerful characteristics of implementing microscopic models as computer simulations is the sheer amount of data that becomes available for analysis. The limitations come from memory and computational power, but not from the simulation itself. Thus, in my implementation of the SM, both velocity-measuring methods can be applied. This is because the simulation keeps track both of the positions of the particles at every timestep, and of the displacements taking place in each unit cell of a virtual, three-dimensional, simple cubic lattice.

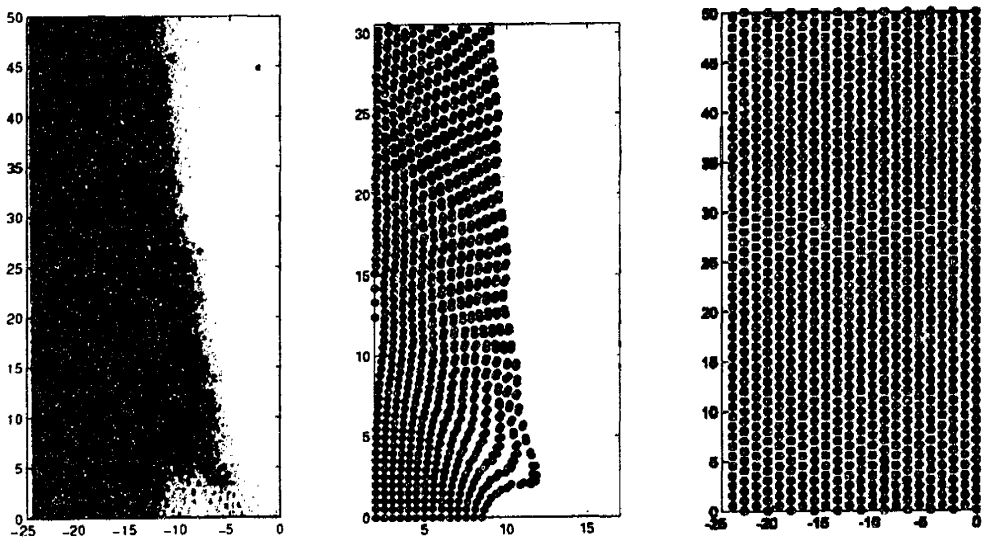

Figure 4: Behavior of an interface in, from left to right, experiment, Spot Model, and Void Model. Whereas the VM wrongly predicts complete loss of the interface, the SM predicts that it will remain sharp and develop a kink near the bottom. The random walk used was a CBN with $\gamma = 0.5$, and the simulation was run for 4,500 timesteps. (Left and right images provided by Martin Bazant.)

5.2 Density Fluctuations

Arguably the most severe problem with simulations of the SM is that, at least with the current implementation, they inevitably lead to unphysicical configurations of particles. Particle density fluctuations will develop in the container such that some regions of empty space develop, whereas other regions become crowded with more particles that could possibly fit there. This problem is illustrated in Figure (5). It was observed that the problem is most striking when the CD random walk is used, and somewhat lessened when using a CBN random walk with relatively high γ (i.e. more than about 0.5.) However, the fluctuation problem persists even for very high γ.

Also in Figure (5) we can observe interesting qualitative features of the granular drainage that are also seen in experiment. Namely, the division of the container into three regions: (1) the region of low x displacement and more-or-less uniform v_z, directly above the orifice; (2) the region of

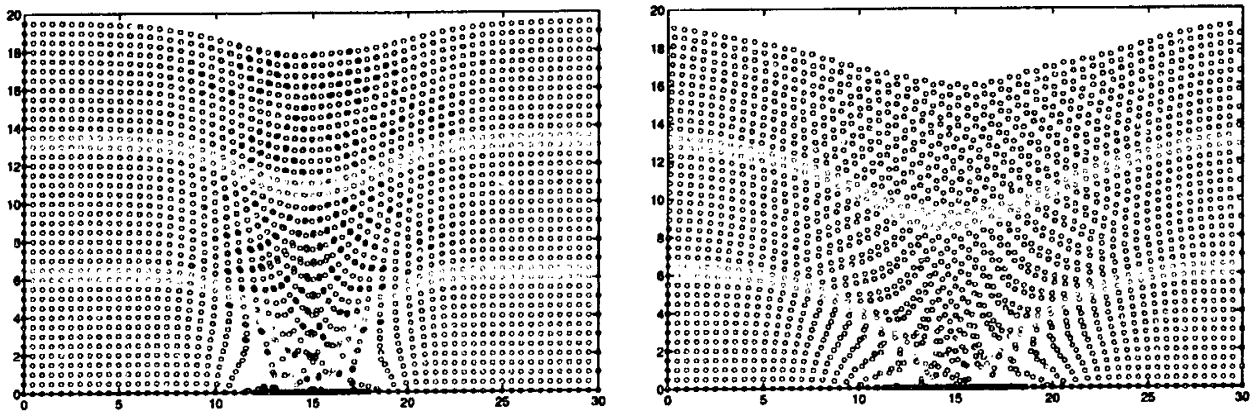

Figure 5: Density fluctuations created by the SM. Both simulations were run for 2,000 timesteps. On the left was used a BN random walk, and on the right a CBN random walk with $\gamma = 0.5$.

highly sheared flow, which extends like a parabola upwards and is where the interfacial kink of Figure (4) forms and where the density fluctuations are most apparent; and (3) the region outside of this parabola, which as we shall see is slow-moving and has low velocity fluctuations.

5.3 Streamlines

Since information about the particle positions at every timestep is available from simulation, the implementation of the SM can be used to measure particle streamlines directly, rather than deriving them from the mean flow profiles (as Caram and Hong did in [1]). I measured particle streamlines with all three different random walks implemented, and with different values of γ for the BCN random walk. Typical plots of the streamlines in these simulations are shown in Figure (6). The surprising result is that for both of the uncorrelated random walks (CD and BN), the streamlines are not parabolic, but rather funnel-shaped. However, as γ increases the curvature of the streamlines increases so that they become more parabolic. This result holds true for both 2D and 3D simulations.

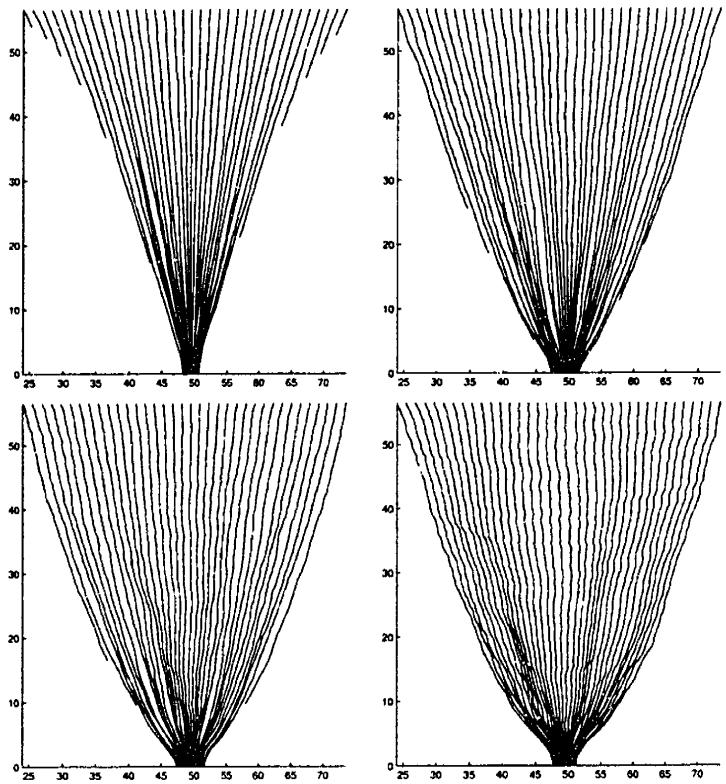

Figure 6: Actual paths traced by particles as they leave the container. Axis units are in particle diameters. Top left was made with a BN random walk. The remaining used a CBN random walk with, in clockwise order, $\gamma = 0.5$, 0.7, and 0.9.

5.4 Particle-following velocity

Particle velocity profiles were measured using a particle-following methodology. An advantage of this method is that we know the exact velocity of each particle. Another advantage is its simplicity: to obtain velocities for a given particle the only computation necessary is

$$\frac{\vec{p}_{\mathrm{p}}^{\,final} - \vec{p}_{\mathrm{p}}^{\,initial}}{n^*}$$

where n^* is either the number of timesteps elapsed at the time the particle leaves the container, or, if the particle has not left the container at the end, the total number of timesteps in the

simulation. There are, however, major disadvantages to this method as well. The most important one is that since the particle changes location, ambiguity arises about how to assign the velocity data to points in space. This makes the data difficult to plot in a natural way. One possible way to work around this is to arbitrarily designate the initial position of the particle as the point that takes that particle's velocity. This scheme was used to generate the plot shown in Figure (7). It is

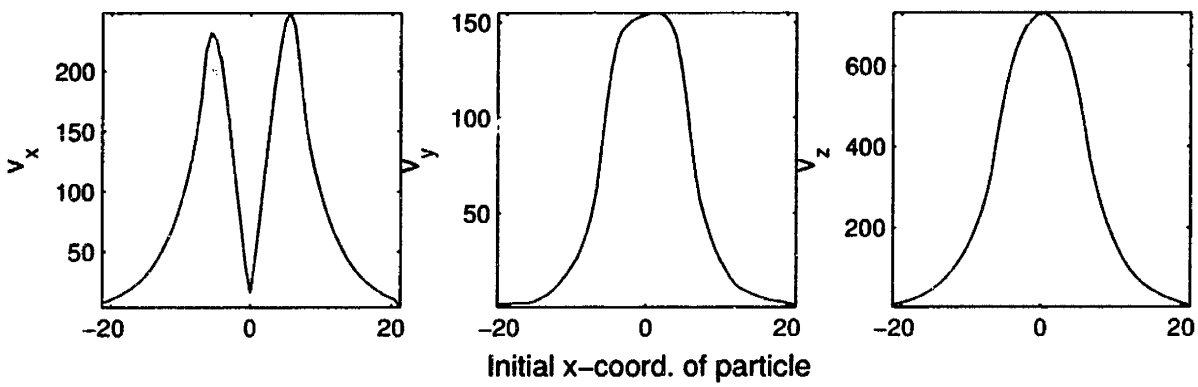

Figure 7: Mean velocity profiles for each component of velocity, averaged over the whole container, obtained from a particle-following perspective. The simulation used a CBN random walk in 3D with $\gamma = 0.5$, and ran for 3,000 timesteps. Units of velocity are not scaled.

reassuring to note that we obtain apparently Gaussian velocity profiles. The reason for the dip in the leftmost plot is that the x component of the velocity will be zero right over the orifice, because those particles will tend on average not to drift laterally.

5.5 Lattice-based velocity

Velocity measurements were also obtained using a lattice, or stationary frame of reference, methodology. This data is more useful than the particle-following data because it can actually be compared to available experimental results. To obtain the results presented in this section, a modified version of the implementation described in section 4 was used. The modification consisted of not allowing

the particles to move. This does not invalidate the measurement of velocity via a static frame of reference: at each timestep, the particle displacements that should take place due to spots are computed in the same way as described in section 4, and these displacements are used to update the data associated with the lattice.

There are two reasons why this modification was used. First of all, the development of density fluctuations invalidates the approximating assumption that $|\mathbb{S}|$ is constant; if the particles are not allowed to move, on the other hand, this assumption is correct. Secondly, the drainage of particles from the container means that as the simulation progresses there will not be any displacements taking place at the top. Again, not allowing the particles to move allows us to more closely simulate the behavior of particles in bulk.

A qualitative comparison between simulation and experimental results, for both the x and z components of the velocity profiles, is shown in Figure (8). These experimental results were obtained by Jaehyuk Choi, using the setup detailed in section 2. Good qualitative agreement with experiment is observed. On the experimental v_z plot, much larger velocities are seen at high z than in the simulation. A possible explanation for this is that the simulations only correspond to short real times, so that not enough time has elapsed for steady-state conditions to be reached at high z.

Since the dynamic aspects of the model were largely ignored in the implementation, The velocity units of the simulation and experimental results are different. In order to compare the two quantitatively, the simulation units must be scaled by an appropiate factor, call it λ. Suppose the container has a mean downward flow rate of particles Q through the orifice. In the steady-state, the mean downward flow rate through any horizontal plane in the container must be equal to Q. If we consider the velocity profile of one of these horizontal planes (i.e. the velocity profile obtained from the lattice at a certain height), then Q corresponds to the area under the profile curve (the velocity profile is a curve and not a surface because the experimental data is 2D). Thus, if we postulate that

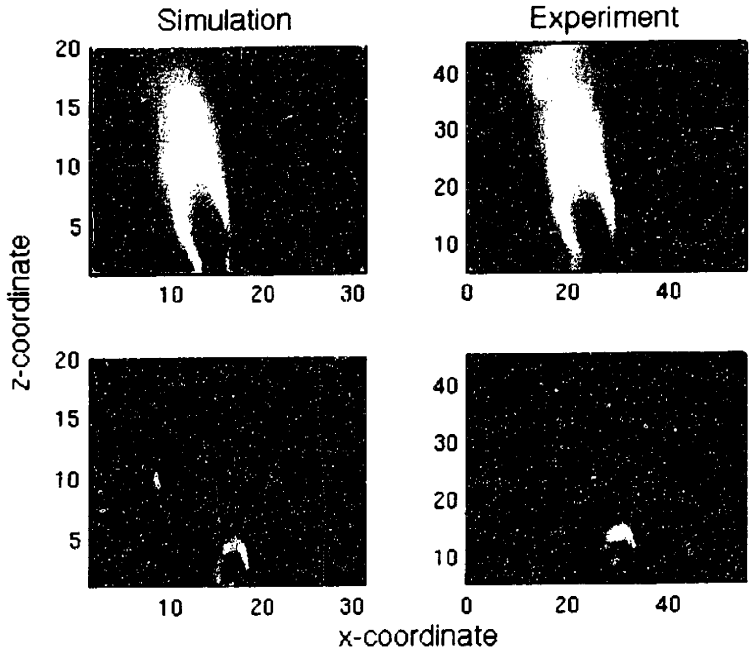

Figure 8: Qualitative comparison of the velocity profiles obtained from experiments and simulations. The simulation was run with a CBN random walk with $\gamma = 0.5$, for 6,000 timesteps. The top graphs show the distribution of v_x in the container, and the bottom graphs show that of v_z. The units of axes on the left does not correspond to that of those on the right.

the mean total flow rate is the same for both experiment and simulation, we obtain the following relation for λ:

$$\lambda = \frac{\int_0^L v_{z,sim} \mathrm{d}x}{Q} = \frac{\int_0^L v_{z,sim} \mathrm{d}x}{\int_o^L v_{z,exp} \mathrm{d}x} \tag{14}$$

so that λ has units of seconds/timestep. This procedure was applied to simulations results obtained using the BN random walk, as well as with the CBN random walk for $\gamma = 0.3$ and 0.5. The results are summarized in Figures (9) and (10). Remarkably good agreement with experiment was obtained when $\gamma = 0.5$. Similar results were also obtained as regards the v_x profiles.

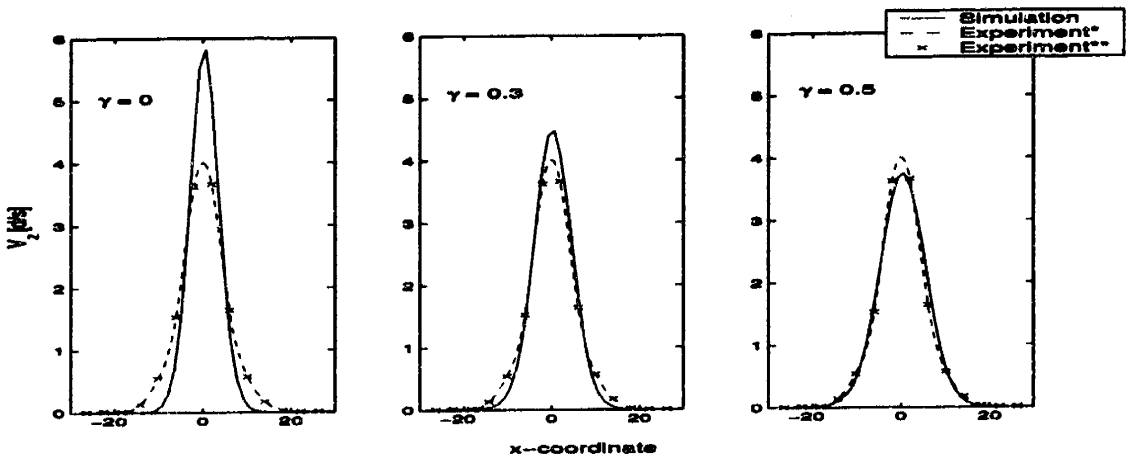

Figure 9: Comparison of velocity profiles with experiment, for different values of γ. The crosses correspond to experimental data points, and the dashed lines to a cubic spline interpolation through those data points. Solid lines are the simulation profiles. The x coordinate is in units of particle diameters, and v_z is in particle diameters per second. Each curve corresponds to the average velocity of particles at a height $z = 7.02$.

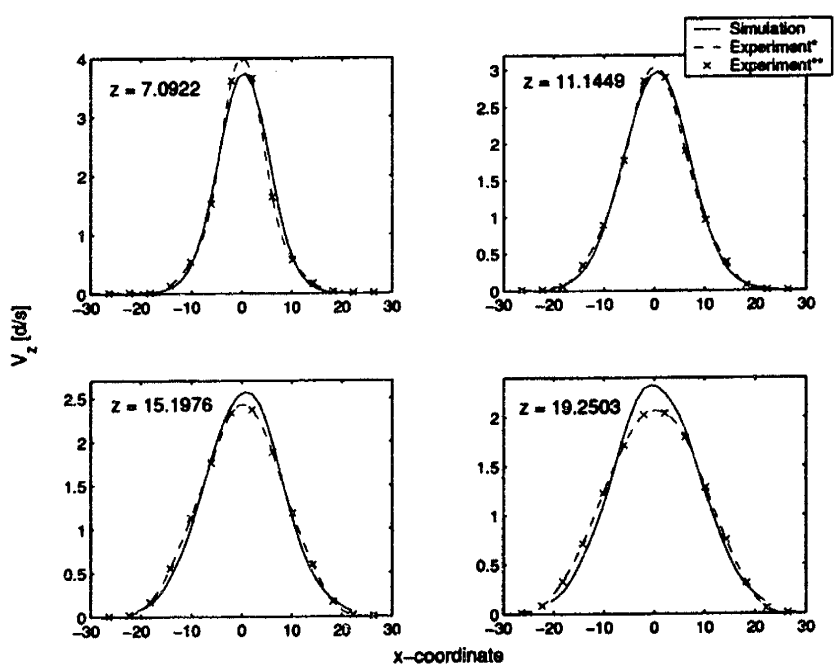

Figure 10: Comparison of velocity profiles with experiment, for $\gamma = 0.5$, at different heights. Units are as in Figure (9).

5.6 Granular Temperature

Thermodynamic temperature is a measure of the average kinetic energy of the system. For solid state materials, it can be understood as an aggregate measure of how large the vibrations or deviations of a molecule are from its equilibrium position. Analogously, granular temperature is a measure of fluctuations in the velocity of particles as they flow. At the microscopic level, it comes about from the random deviations a particle has from its predicted streamline out of the container. In discrete terms, we can think of it as $\vec{d}_{\mathrm{p}}$ minus the displacement predicted by the mean flow at $\vec{p}_{\mathrm{p}}$. It is an interesting quantity to measure because it is related to the diffusivity and mixing of particles: if we can measure the granular temperature at different parts of our system, then we can know where the most mixing takes place.

I used a static-frame-of-reference (as opposed to particle-following) methodology to study the granular temperature of the system. In this scenario, granular temperature can be defined as the standard deviation of the velocity. In practical terms, I measured this quantity by keeping track, at each timestep, not only of the displacements that take place in each unit of the velocity-measuring lattice, but also of the squares of those displacements. The relation for variance can then be applied: $\mathrm{Var(X)} = \langle \mathrm{X}^2 \rangle - \langle \mathrm{X} \rangle^2$, and standard deviation is just the square root of the variance. This method can be used to produce a map of the granular temperature in the container. A typical example is shown in Figure (11). Unfortunately at the time of this writing there are no available experimental results to compare against Figure (11).

It is also possible to measure the dependence of the standard deviation of v_x, the horizontal component of the velocity, on v_z, the vertical component. This is obtained, essentially, from comparison of results such as those from Figure (8) with results such as those from Figure (11). Each unit in the lattice yields a data point. This dependence is plotted in Figure (12) for a typical

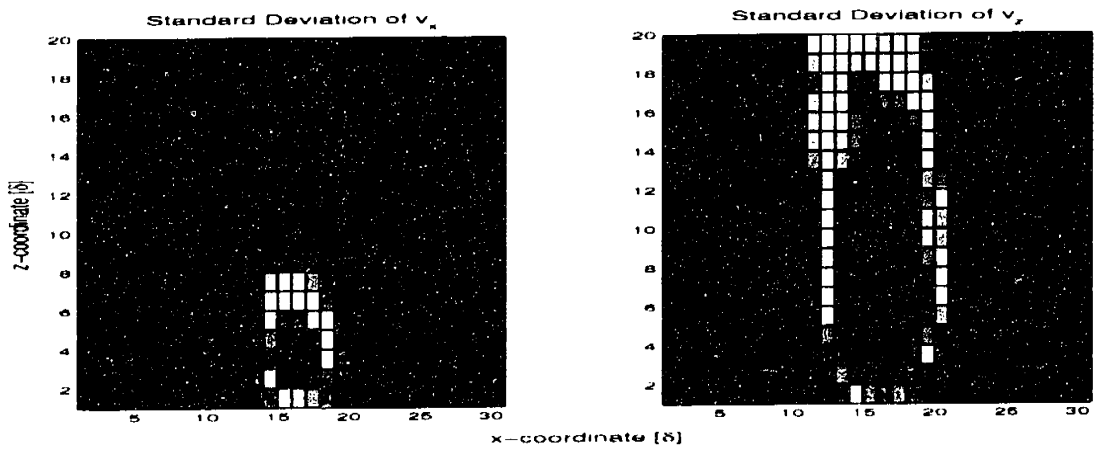

Figure 11: Plot of the standard deviation of v_z and v_x in the container. The axes are in units of particle diameters/$\sqrt{2}$

simulation run. An interesting feature to note is that there are clearly distinct curves present in the plot, but every curve in the log-log plot seems, at a glance, to have the same slope. Choi carried out experiments to measure a similar dependence of standard deviation on v_z. His methodology is different, however, so his results might not be comparable to the simulation. Choi utilized a lattice-based methodology, but rather than look at the whole container, he focused on a small region centered above the orifice and at large z. The v_z profile in this region is almost uniform [2]. By varying the width of the orifice, v_z can be controlled, and the standard deviation of v_x measured. The dependence obtained was apparently linear, with a slope of about 0.2. However, if we look at the linear plot of Figure (??), we see that drawing a best-fit line to the curves and taking the slope would also yield a slope of about 0.2.

[2] A feature not observed in simulations, presumably because so far only comparatively low container heights have been used, due to computational constraints

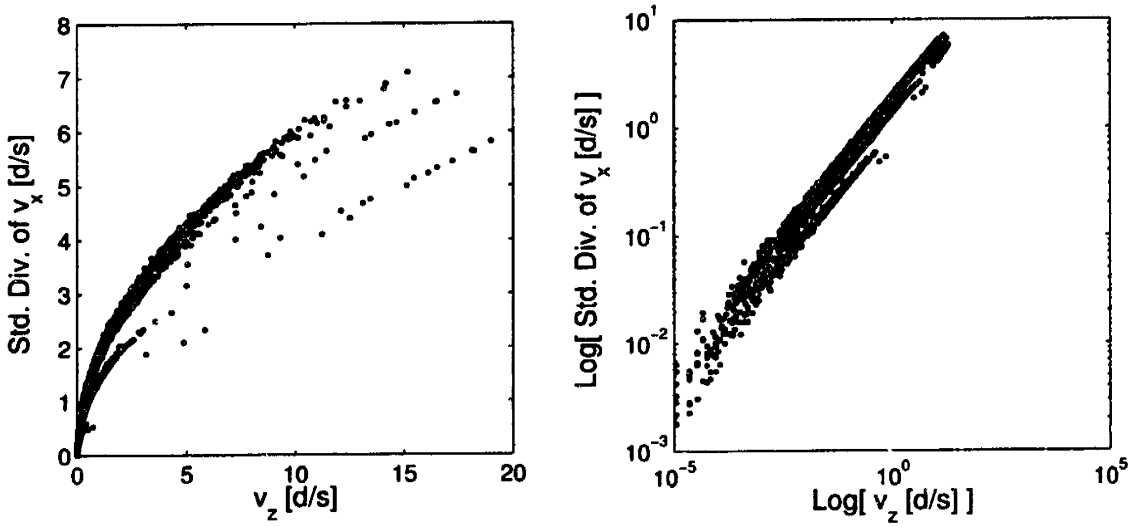

Figure 12: Linear and Log-Log plots of the relation between standard deviation of v_x, and v_z. Velocities are measured in units of particle diameters per second, and where scaled using $\lambda = 2{,}500$.

6 Discussion & Conclusions

Several interesting results were presented in the previous section. In the following sections I will discuss what I believe are some of the more salient features of the results, and some of the conclusions we can derive from them.

6.1 Running Time of the Simulation

Almost as an aside, note that a typical value of λ from a CBN simulation run is about 2,500. This means that it takes roughly 2,500 timesteps to simulate 1 second of real time. On a reasonably powerful personal computer, it takes about 25 minutes to simulate 40,000 particles for 2,500 timesteps. This is encouraging, because it means that with improvements to the code, and by running the simulation on a more powerful computer, it would be possible to simulate hundreds of thousands of particles for extended periods of real time. In other words, it starts to become possible to simulate

real systems for real applications [2].

6.2 Random Walks

It is clear that there is very strong evidence supporting the notion that the CBN random walk is closest to what occurs in experiments. First of all, it is observed that the CBN helps reduce the density fluctuation problem more than the other two random walks. Secondly, Both the CD and BN random walks have particle streamlines that resemble straight lines more than parabolas, whereas the CBN displays parabolic streamlines, that moreover increase in curvature with increasing correlation γ. Thirdly, The excellent agreement with experiment shown in Figure (10) was only achieved when a CBN random walk was used. For these reasons, it seems that a correlated walk of some sort is necessary for the proper functioning of the Spot Model, and the CBN in particular presents a strong candidate.

6.3 Density Fluctuations

The main problem with the computer simulation of the SM, that it cannot be used to obtain realistic arrangements of particles in the container, remains largely unresolved. Although using a correlated walk reduces the problem somewhat, it still becomes apparent after a few thousand timesteps of simulation. However, considering that the particles are not restricted to lie on a lattice, as in the VM, it is not surprising that density problems develop. As noted in section 4.1, little is known about generating valid close-packed arrangements of particles. If the SM managed somehow to maintain uniform density, it would be worth studying for this reason alone.

Despite this problem, however, the SM can still be used to obtain meaningful results. It is my opinion that the density fluctuations will not pose a problem to further comparison of simulation and experimental results of many features of the flow, such as granular temperature and direct

measurements of particle diffusivity.

6.4 Granular Temperature

The results depicted in Figure (12) are somewhat difficult to interpret, in part because I know of no theory describing the behavior of velocity fluctuations in granular drainage, and also in part because of the scarcity of experimental results in this are. With regard to Choi's experimentally observed linear dependence with slope 0.2, I believe two interpretations are possible, and I do not know which is more likely. First, it is possible that Choi's results differ from mine (linear vs. logarithmic) because we are not really measuring the same dependence (uniform region/whole container and v_z varied by hole width/variation of v_z present in container.) The second possibility is that Choi's data really reflects the approximately-linear shape of the logarithmic curve away from the origin.

It is, of course, to be expected that as v_z increases so do the fluctuations of v_x. However, the origins of the logarithmic dependence are unclear. I find the fact that there are distinct lines present in Figure (12) highly interesting. Each line corresponds to a different region of the container, and possibly indicates the presence of different regimes of granular flow. Although I have not yet determined the geometric correspondence between lines in this Figure, and regions of the container, it is my expectation that this correspondence will be closely related to the regions discussed in section 5.2.

In summary, then, it is possible either that: Choi's results (linear with slope 0.2) are qualitatively different from mine because

6.5 Conclusions

Based on the excellent agreement with experiment seen by various different measures, such as the mean flow profiles, the parabolic streamlines (which were measured directly), and the prediction of particle mixing, I would strongly recommend the Spot Model over any other model of granular drainage, at least for applications where a microscopic model, and knowledge about the detailed behavior of particles, is desired. There is much further research to be made for the better establishment and refinement of the Spot Model, as I detail in the next section, but these initial results are highly encouraging.

Besides accurate predictions that can be applied to real problems, a model is only really as good as the physical insight it yields about the phenomenon at hand. This is one reason, I believe, the molecular dynamics type models have been unsuccessful in this field. I feel that the notion of spots does indeed provide some insight into the workings of granular flow, and I hope to see this insight used in the future to tackle problems beyond the simple setup of drainage from a silo.

7 Future Research

The SM is a brand-new model, and there are many available avenues of research. There are some basic results that could be obtained with the existing implementation of the Spot Model, but were not obtained due to time constraints. Probably the highest priority in this category is measurement of the particle diffusivity. Both the average particle diffusivity, and the behavior of individual particles, are of interest. Also, the dependences of diffusion length on time, and of diffusivity on v_z, can both be measured with the existing implementation. In fact, computer simulation makes it possible to approach these questions from both a lattice-based and a particle-following methodology. Diffusion and diffusivity are of interest because there are some existing experimental results that could be used for comparison, and also because previous models have tended to fare badly in predicting them.

Another aspect of the model that deserves further research is that of granular temperature. I believe that ultimately, the idea of mapping out granular temperature in a container using the SM could have useful applications in industry. In particular, development in this area should be in done in conjunction with the acquisition of relevant experimental results. It would be interesting to study the notion of granular temperature from a particle-following perspective as well, i.e. looking at the deviations from the mean of each displacement in a particle's path. This would be possible with the existing implementation of the model.

Going beyond what is possible with the current implementation, I identify two major areas of research: dynamics and boundary regions. With respect to dynamics, there are some known relations that can be incorporated into the model with relative ease, such as the relation between Q and the width of the orifice. But there are many unanswered questions about both spot and particle dynamics. How many spots are in the container at any one time, and how are they distributed?

Do they interact with each other? Studying these questions, we could begin to model not just the velocity, but also the acceleration profiles of the particles, as well.

With respect to boundary regions, the region of interest is, of course, the free surface. The goal here would be to reproduce the angle of repose as Caram and Hong did [1]. This could possibly be accomplished with an approach as simple as theirs was, forcing the spot to continue to propagate along the free surface once it reaches it. The behavior of spots against walls of different roughnesses and curvature can also be studied.

For the study of both dynamics and boundary regions, a useful tool to keep in mind is, as I mentioned earlier, the influence function, w. Tailoring this function will be, I believe, a primary mean of affecting the spot's behavior.

Acknowledgments

I would like to extend my sincere gratitude to Martin Bazant for developing the model that is the subject of this thesis, for extending to me an invitation to work on the model, and for providing much helpful discussion; but most of all for his patience with my untimeliness and disorganization. I would also like to thank Jaehyuk Choi for contributions to the project and for the hours of his time dedicated to helping me understand the model and his experimental results. Finally, I would like to thank my girlfriend, Avni Shah, for support when I most needed it.

References

[1] H. Caram and D. C. Hong, *Random-Walk Approach to Granular Flows*, Physical Review Letters, Volume 67, Number 7 (1991)

[2] J. Choi et al, *Pebble Dynamics in PBMR: Experiments and Modeling*, Unpublished, Project Report for 22.033, Dept. of Nuclear Engineering, Massachussetts Institute of Technology. (2002)

[3] M. Bazant, *Statistical Dynamics of Granular Drainage*, To be published (2002).

[4] J. Litwiniszyn, *The model of a random walk of particles adapted to researchers on problems of mechanics of loose media*, Bull. Acad. Po. Sci., 11, 593 (1963)

[5] W. W. Mullins, *Stochastic Theory of Particle Flow Under Gravity*, Journal of Applied Physics, Volume 43, Number 2. (1972)

[6] W. W. Mullins, *Critique and Comparison of Two Stochastic Theories of Gravity-Induced Particle Flow*, Powder Technology, 23, 115-119. (1979)

[7] R. M. Nedderman and U. Tüzün, *A Kinematic Model for the Flow of Granular Materials*, Powder Technology, 22, 243-253. (1979)

[8] D. Hirshfeld, Y. Radzyner and D. C. Rapaport, *Molecular Dynamics Studies of Granular Flow Through an Aperture*, Physical Review E, Volume 56, Number 4. (1997)

[9] E. Weisstein, *World of Mathematics*, http://www.mathworld.com

THESIS PROCESSING SLIP

FIXED FIELD: ill. _____ name _____

index _____ biblio _____

► **COPIES:** (Archives) Aero Dewey Barker Hum

Lindgren Music Rotch Science Sche-Plough

TITLE VARIES: ► ☐ _____

_____

_____

NAME VARIES: ► ☑ Richard _____

_____

IMPRINT: **(COPYRIGHT)** _____

_____

► **COLLATION:** _____

_____

► **ADD: DEGREE:** S.B. ► **DEPT.:** Math

► **ADD: DEGREE:** _____ ► **DEPT.:** _____

SUPERVISORS: _____

_____

NOTES:

cat'r: date:

page: ▶ J6+31

► **DEPT:** Mat Sci & E.

► **YEAR:** 2003 ► **DEGREE:** S.B.

► **NAME:** GUAQUETA, Camilo R.

_____